Quest Journals
Journal of Research in Applied Mathematics
Volume 12 ~ Issue 9 (September 2026) pp: 13-23
ISSN (Online): 2394-0743 ISSN (Print): 2394-0735
www.questjournals.org

Research Paper

Fourier Integral Transform Solutions for Stationary Oscillation Problems in Micropolar Elastic Half-Planes, Strips, and Layers

Hashim Mohammed Mukhtar
Supervisor: Dr. Adel Ahmed Hassan Kubba

Abstract
This study presents a unified analytical formulation based on the Fourier integral transform for solving stationary oscillation problems in isotropic linear micropolar elastic media. The formulation incorporates independent microrotation, asymmetric force stresses, and couple stresses in addition to the conventional displacement field. The methodology is developed for three representative configurations: the elastic half-plane, finite elastic strip, and finite elastic layer. For the principal layer problem, the governing equations are transformed into the Fourier domain and reduced to a coupled system of ordinary differential equations. A characteristic-matrix formulation is then employed to determine the admissible modes, modal vectors, and unknown boundary coefficients. The resulting solution provides the displacement, microrotation, force-stress, and couple-stress fields. Numerical evaluation is performed for a representative reference case and compared with the corresponding classical elastic response. The results demonstrate substantial differences between the micropolar and classical predictions, including reduced translational displacement, modified stress distributions, and a localized microrotational response. The formulation provides an analytical benchmark for numerical implementations and for the analysis of microstructured elastic media under stationary harmonic loading.

Keywords: *Micropolar elasticity; Fourier integral transform; stationary oscillation; elastic layer; microrotation; couple stress; characteristic modes; size effects.*

Received 11 Sep., 2026; Revised 19 Sep., 2026; Accepted 21 Sep., 2026 © The author(s) 2026. Published with open access at ***www.questjournals.org***

I. Introduction

The analysis of wave propagation and stationary oscillation phenomena in elastic media is of fundamental importance [1], [2] in solid mechanics, structural engineering, geomechanics, and materials science. Analytical solutions remain particularly valuable because they provide direct insight into the governing physical mechanisms and constitute reference solutions for validating numerical models.

Classical elasticity provides an effective framework for describing deformation and stress in conventional homogeneous solids [1]–[3]. However, its assumption that each material point possesses only translational degrees of freedom becomes restrictive when the characteristic dimensions of a structure approach the intrinsic length scale of its microstructure. Granular materials, cellular solids, lattice structures, fiber-reinforced composites, foams, metamaterials, and other microstructured materials may exhibit particle rotations, couple stresses, and size-dependent responses that are not represented adequately by the classical theory.

Micropolar elasticity extends the classical continuum by introducing independent microrotational degrees of freedom together with asymmetric force stresses and couple stresses [4]–[6]. This generalized description captures translational–rotational interactions associated with material microstructure.

Previous studies have considered wave propagation, stress concentration, crack problems, and boundary-value problems in micropolar media using integral transforms, eigenfunction expansions, potential methods, and numerical techniques [4]–[7], [10]–[16]. The Fourier integral transform is particularly effective for unbounded and layered domains because it converts differentiation along an infinite spatial direction into algebraic operations while retaining the analytical structure of the problem.

The present study develops a unified Fourier-transform formulation for stationary oscillation problems in micropolar elasticity and applies it to the half-plane, strip, and finite-layer configurations. Particular attention is given to the finite layer, for which the complete modal and boundary-value solution is evaluated numerically.

Novelty and Contributions

The main novelty of this work lies in the development of a unified analytical framework that combines Fourier integral transformation, characteristic-mode analysis, and an independent boundary-matrix formulation for stationary oscillations in micropolar elastic media.

The principal contributions are:

1. A unified Fourier-domain formulation applicable to micropolar elastic half-planes, strips, and finite layers.
2. A systematic characteristic-matrix formulation for determining the admissible characteristic roots and associated modal vectors.
3. A separate boundary-matrix formulation for determining the modal coefficients required to satisfy the prescribed mechanical and couple-traction boundary conditions.
4. A complete reconstruction of displacement, microrotation, force-stress, and couple-stress fields from the transformed solution.
5. A numerical reference solution for a finite micropolar layer together with a direct comparison against the corresponding classical elastic response.
6. Identification of the non-monotonic displacement and microrotation distributions in the selected finite-layer reference configuration, demonstrating the coupled translational–rotational response associated with micropolar elasticity.

The paper is organized as follows. Section 2 presents the mathematical formulation. Section 3 develops the Fourier-transform and characteristic-matrix methodology. Section 4 summarizes the analytical solutions for the three geometries, with emphasis on the finite layer. Section 5 presents the numerical implementation and reference results. Section 6 discusses engineering implications and conclusions.

II. Mathematical Formulation

The analysis considers a homogeneous, isotropic, linear micropolar elastic medium undergoing small deformation and small microrotation. The material occupies a domain infinite in the x-direction, with the layer-normal coordinate denoted by y. The finite layer therefore occupies

$$x \in (-\infty, \infty), \qquad 0 \le y \le h.$$

The displacement field is
and the two-dimensional micropolar formulation contains one independent microrotation,

$$u = (u, v, 0), \qquad \phi = (0, 0, \phi).$$

The micropolar strain measures are

$$\gamma_{xx} = \partial u/\partial x, \quad \gamma_{yy} = \partial v/\partial y,$$

$$\gamma_{xy} = \partial u/\partial y - \Phi, \quad \gamma_{yx} = \partial v/\partial x + \Phi.$$

The curvature measures associated with microrotation are

$$\kappa_{zy} = \frac{\partial \phi}{\partial y}, \qquad m_{yz} = \gamma \frac{\partial \phi}{\partial y}.$$

The force-stress tensor is expressed through the micropolar constitutive law:

$$\sigma_{ij} = \lambda \gamma_{kk} \delta_{ij} + (\mu + \kappa)\gamma_{ij} + \mu \gamma_{ji}.$$

The couple-stress relation above is the definition used in the boundary conditions and numerical reconstruction.

The curvature-related coefficient gamma governs the couple-stress response associated with gradients of microrotation. In the present two-dimensional formulation,

DOI: 10.35629/0743-12090112

the couple-stress component used in the boundary conditions is given by:

$$m_{yz} = \gamma \, \partial\Phi/\partial y$$

The equations of linear and angular momentum provide the coupled translational and rotational governing equations. The micro-inertia parameter is denoted by J. The harmonic stationary response is represented using

$$\partial_t f = -i\omega f, \qquad \partial_t^2 f = -\omega^2 f.$$

Thus, the inertial terms enter the translational and rotational equations through $-\rho\omega^2$ and $-J\omega^2$, respectively.

$$f(x, y, t) = \hat{f}(x, y)e^{-i\omega t}.$$

For consistency throughout the present paper, x denotes the horizontal coordinate, y the layer-normal coordinate, β the Fourier wave number, κ the micropolar coupling modulus, γ the couple-stress coefficient, η the curvature coefficient entering the characteristic rotational coefficient, and J the micro-inertia parameter. The symbols β and κ are not used interchangeably with k or other alternative wave-number/coupling notation.

$$\widehat{\partial_x f} = i\beta\hat{f}.$$

$$\hat{f}(\beta, y) = \int_{-\infty}^{\infty} f(x, y)e^{-i\beta x}\, dx, \quad f(x, y) = \frac{1}{2\pi}\int_{-\infty}^{\infty} \hat{f}(\beta, y)e^{i\beta x}\, d\beta.$$

The Fourier transform convention follows the standard integral-transform framework [8], [9].

This convention and the distinct roles of β and κ are retained throughout the formulation.

For the finite layer, the lower surface is subjected to a prescribed normal traction, while the remaining prescribed boundary quantities are zero. The upper surface is traction- and couple-traction-free. In the transformed problem, the boundary conditions are:

$$\hat{\sigma}_{xy}(\beta, h) = 0, \quad \hat{\sigma}_{yy}(\beta, h) = 0, \quad \hat{m}_{yz}(\beta, h) = 0.$$

$$\hat{\sigma}_{xy}(\beta, 0) = 0, \quad \hat{\sigma}_{yy}(\beta, 0) = \bar{P}(\beta), \quad \hat{m}_{yz}(\beta, 0) = 0.$$

while the remaining boundary conditions have zero prescribed values.

III. Fourier Integral Transform Solution

3.1 Transformed Governing System

The transformed fields are represented by the exponential modal ansatz used to define the characteristic modes.

Substitution of this ansatz produces the homogeneous algebraic system K(q,beta,omega)a = 0.

A_1 is defined by

$$A_1 = (\lambda + 2\mu + \kappa)\beta^2 - \rho\omega^2.$$

A_2 is defined by

$$A_2 = (\mu + \kappa)\beta^2 - \rho\omega^2.$$

A_3 is defined by

$$A_3 = \eta\beta^2 + 4\kappa - J\omega^2.$$

The coefficient definitions above are used directly in the characteristic matrix.
The implementation in characteristic_equation.py uses exactly these definitions.

3.2 Characteristic Modes
For each characteristic mode, the transformed fields take the exponential form

$$[\hat{U}, \hat{V}, \hat{\Phi}]^T = \mathbf{a}\, e^{-qy}$$

$$\mathbf{K}(q, \beta, \omega)\, \mathbf{a} = \mathbf{0}$$

Substitution of this ansatz gives the homogeneous algebraic system
The characteristic matrix is defined by

$$K_{11} = (\mu + \kappa)q^2 - A_1, \quad K_{12} = -i\beta q(\lambda + \mu), \quad K_{13} = 2\kappa q$$

$$\mathrm{K} = \qquad K_{21} = -i\beta q(\lambda + \mu), \quad K_{22} = (\lambda + 2\mu + \kappa)q^2 - A_2, \quad K_{23} = 2i\beta\kappa$$

$$K_{31} = 2\kappa q, \quad K_{32} = -2i\beta\kappa, \quad K_{33} = \gamma q^2 - A_3.$$

This matrix is implemented directly in characteristic_equation.py.
The characteristic equation is

$$\det K(q, \beta, \omega) = 0.$$

Because the determinant is even in q, the admissible attenuation roots occur in six modal branches for the finite-layer calculation.

$$q_1, q_2, \ldots, q_6, \qquad K(q_j, \beta, \omega)a_j = 0.$$

For each root, the corresponding modal vector satisfies
For the half-plane, the medium extends indefinitely in the positive y-direction. Boundedness therefore requires retention of the modes satisfying the appropriate decay condition.

$$[\widehat{U}, \widehat{V}, \widehat{\Phi}]^T = \sum_{j=1}^{6} C_j a_j e^{-q_j y}, \qquad a_j = [U_j, V_j, \Phi_j]^T.$$

3.3 Boundary-Condition System
The six boundary conditions are imposed at y=0 and y=h:

$$\widehat{\sigma}_{xy}(\beta, h) = 0, \quad \widehat{\sigma}_{yy}(\beta, h) = 0, \quad \widehat{m}_{yz}(\beta, h) = 0.$$

$$\widehat{\sigma}_{xy}(\beta, 0) = 0, \quad \widehat{\sigma}_{yy}(\beta, 0) = \bar{P}(\beta), \quad \widehat{m}_{yz}(\beta, 0) = 0.$$

The six boundary equations are assembled into the finite boundary-matrix system:

$$B(\beta, \omega, h)C = F(\beta), \qquad C = [C_1, \ldots, C_6]^T, \qquad F = [0, \bar{P}, 0, 0, 0, 0]^T.$$

where C contains the six modal coefficients and F contains the transformed loading terms.

Provided that the boundary matrix is nonsingular, the modal coefficients are uniquely determined.

The resulting coefficients are then used for field reconstruction.

IV. Analytical Solutions for the Considered Geometries

The general Fourier-domain solution provides a common mathematical basis for the three configurations considered: the micropolar elastic half-plane, finite strip, and finite layer.

For the half-plane, the medium extends indefinitely in the positive y-direction. Boundedness therefore requires retention of the modes satisfying the appropriate decay condition,

The half-plane serves as a reference configuration for the finite geometries.

The finite layer is the principal configuration investigated numerically. It occupies

$$x \in (-\infty, \infty), \qquad 0 \le y \le h.$$

and is subjected to harmonic normal loading at one surface while the opposite surface is traction-free.

The six modal coefficients are determined from the boundary-matrix system:

$$B(\beta, \omega, h)C = F(\beta), \qquad C = [C_1, \ldots, C_6]^T, \qquad F = [0, \bar{P}, 0, 0, 0, 0]^T.$$

The physical displacement, microrotation, stress, and couple-stress fields are then recovered through the inverse Fourier transformation:

$$f(x, y) = \frac{1}{2\pi}\int_{-\infty}^{\infty} \hat{f}(\beta, y)e^{i\beta x}\, d\beta.$$

The corresponding physical stress and couple-stress fields are obtained by applying the same inverse transform to their transformed counterparts.

V. Numerical Implementation and Results

5.1 Computational Framework

The numerical implementation follows the sequence

The characteristic matrix is evaluated for the selected Fourier wave number β and angular frequency ω; the six roots are determined, the modal vectors are obtained, and the boundary matrix is assembled. The resulting modal coefficients are then used to reconstruct the transformed fields.

The implementation was checked against the characteristic matrix and the prescribed boundary conditions. The program explicitly uses K(q,β,ω) as the characteristic matrix.

5.2 Reference Material and Geometric Parameters

Numerical reproducibility. The reported finite-layer reference calculation uses $\lambda = 2.5 \times 10^9$ Pa, $\mu = 1.2 \times 10^9$ Pa, $\kappa = 0.6 \times 10^9$ Pa, $\gamma = 8.0 \times 10^{-3}$ N, $\eta = 8.0 \times 10^{-3}$ N, $\rho = 2200$ kg/m³, $J = 1.0 \times 10^{-6}$ kg·m, h = 1 m, β = 2 m^{-1}, and ω = 10 rad/s. The computational Fourier grid spans $0 \le \beta \le 40\ m^{-1}$ with 400 samples; the spatial grid uses $x \in [-5,5]$ with 201 points and $y \in [0,h]$ with 101 points. The verified boundary calculation uses the normalized transformed normal load $\bar{P} = 1$, while the physical input amplitude in the numerical input file is $P_0 = 10^5$ Pa; the prescribed shear and couple loads are $T_0 = 0$ and $M_0 = 0$. These settings define the reproducible reference configuration without altering the previously closed analytical or numerical results.

The final reference case is

Parameter	**Symbol**	**Value**	**Unit**
Lamé constant	λ	2.5×10^9	Pa
Shear modulus	μ	1.2×10^9	Pa
Micropolar coupling modulus	κ	0.6×10^9	Pa
Curvature coefficient	γ	8.0×10^{-3}	N
Density	ρ	2200	kg/m³
Layer thickness	h	1	m
Fourier wave number	β	2	m^{-1}

Parameter	Sym	Value	Unit
Angular frequency	ω	10	rad/s
Normalized transformed	$\bar{P}$	1	—
Curvature coefficient used	η	8.0×10^{-3}	N
Micro-inertia parameter	J	1.0×10^{-6}	kg·m

The characteristic length is defined by

$$\ell = \sqrt{\gamma/\mu}$$

This distinction is essential for consistency between the physical loading definition and the normalized transformed calculation. The same reference convention is used throughout the reported numerical tables and comparisons.

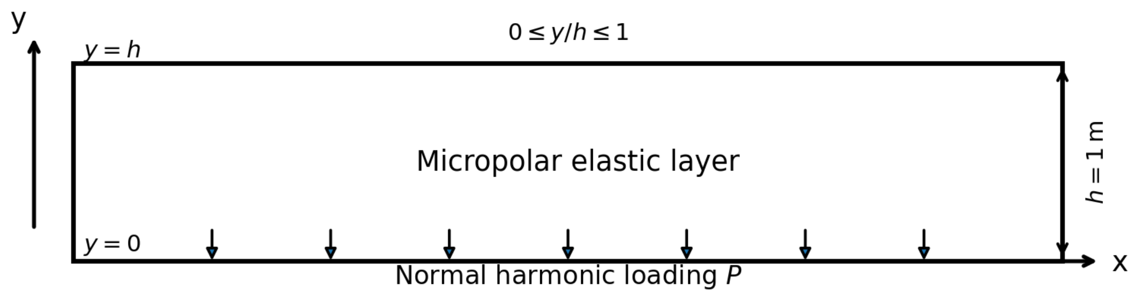

Figure 1. Reference finite-layer geometry, coordinate system, and normalized surface loading.

5.3 Displacement Distribution

For the reference case, Figure 2 shows the corresponding displacement-amplitude profiles.

For the reference case, the computed micropolar displacement amplitude decreases from $4.3602354 \times 10^{-11}$ at y/h = 0 to $4.9575974 \times 10^{-12}$ at y/h = 0.20, and subsequently increases to $9.8393427 \times 10^{-11}$ at y/h = 1.

$$|U|_{\text{micro}}(0) = 4.3602354 \times 10^{-11}$$
$$|U|_{\text{micro}}(0.20) = 4.9575974 \times 10^{-12}$$
$$|U|_{\text{micro}}(1) = 9.8393427 \times 10^{-11}$$

The corresponding classical solution reaches a minimum displacement amplitude of $1.3737680 \times 10^{-10}$ at y/h = 0.40 and increases to 8.9527666×10^{-9} at y/h = 1.

$$|U|_{\text{classical}}(0.40) = 1.3737680 \times 10^{-10}$$

$$|U|_{\text{classical}}(1) = 8.9527666 \times 10^{-9}$$

The important conclusion is that the computed finite-layer profile is **non-monotonic**. Therefore, the numerical results do not support a statement that the displacement amplitude simply decays monotonically through the entire layer.

The pointwise displacement ratio between the micropolar and classical solutions ranges from approximately 0.16% to 23.20%, with the maximum ratio occurring at y/h = 0.40.

$$0.16\% \le 100\,|U|_{\text{micro}}/|U|_{\text{classical}} \le 23.20\%$$

$$\text{max ratio occurs at } y/h = 0.40$$

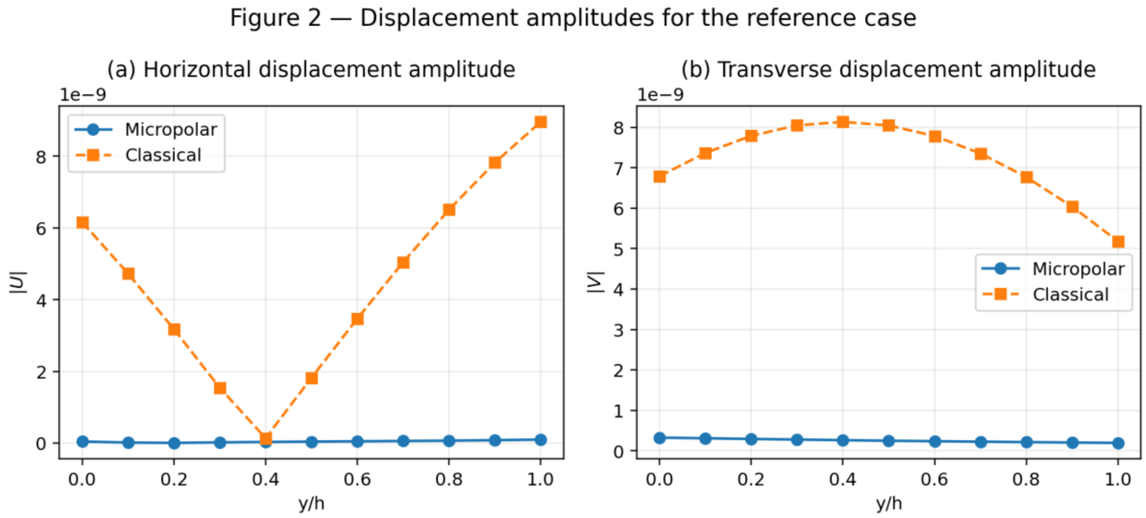

Figure 2. Displacement amplitudes through the finite micropolar layer for the reference case: (a) horizontal displacement U and (b) transverse displacement V, with classical comparison.

5.4 Stress Distribution

The numerical stress analysis compares the force-stress fields predicted by the classical and micropolar formulations under identical conditions. The resulting stress profiles are shown in Figure 3.

The micropolar formulation introduces additional coupling between translational deformation and microrotation. Consequently, the force-stress field differs from the corresponding classical solution, particularly in regions where the rotational response is appreciable. The computed results show modified stress gradients and a redistribution of the force-stress response associated with the coupled force- and couple-stress system.

The shear-stress field shows a pronounced modification relative to the classical reference solution in the selected configuration.

Because the micropolar force-stress tensor is generally asymmetric, the shear response also reflects the rotational degree of freedom that is absent from classical elasticity.

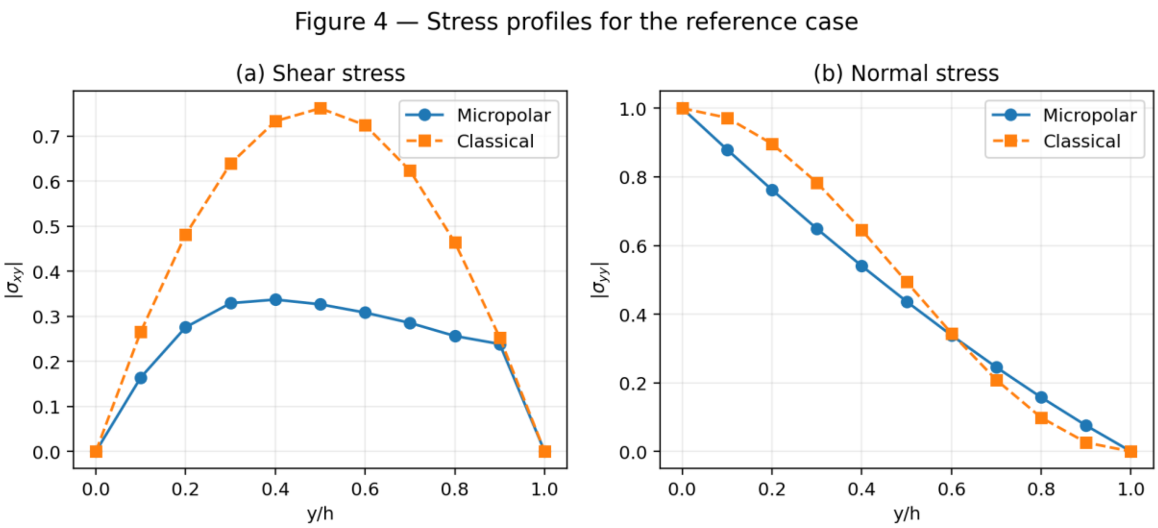

Figure 3. Stress profiles through the layer for the reference case: (a) shear stress sigma_xy and (b) normal stress sigma_yy, with classical comparison.

5.5 Microrotation Field

Independent microrotation is a defining feature of the micropolar formulation. For the selected reference configuration, the numerical solution exhibits a nonzero rotational response throughout the finite layer. The microrotation amplitude increases from $|\Phi(0)| = 1.619 \times 10^{-10}$ at the loaded surface to a maximum of approximately $|\Phi|max = 2.096 \times 10^{-10}$ at $y/h \approx 0.30$, and subsequently decreases toward the opposite surface, where $|\Phi(1)| = 9.627 \times 10^{-11}$. The computed microrotation profile is shown in Figure 4.

Thus, the rotational response is concentrated in a near-surface interior region rather than attaining its maximum exactly at the loaded boundary. This non-monotonic behavior reflects the coupled interaction between translational deformation, microrotation, and the characteristic modes of the finite layer.

The microrotation field is directly coupled to the displacement and stress fields and represents a mechanical degree of freedom that is absent from classical elasticity. In the appropriate classical limiting formulation, where the micropolar rotational effects are suppressed, the independent microrotation contribution vanishes.

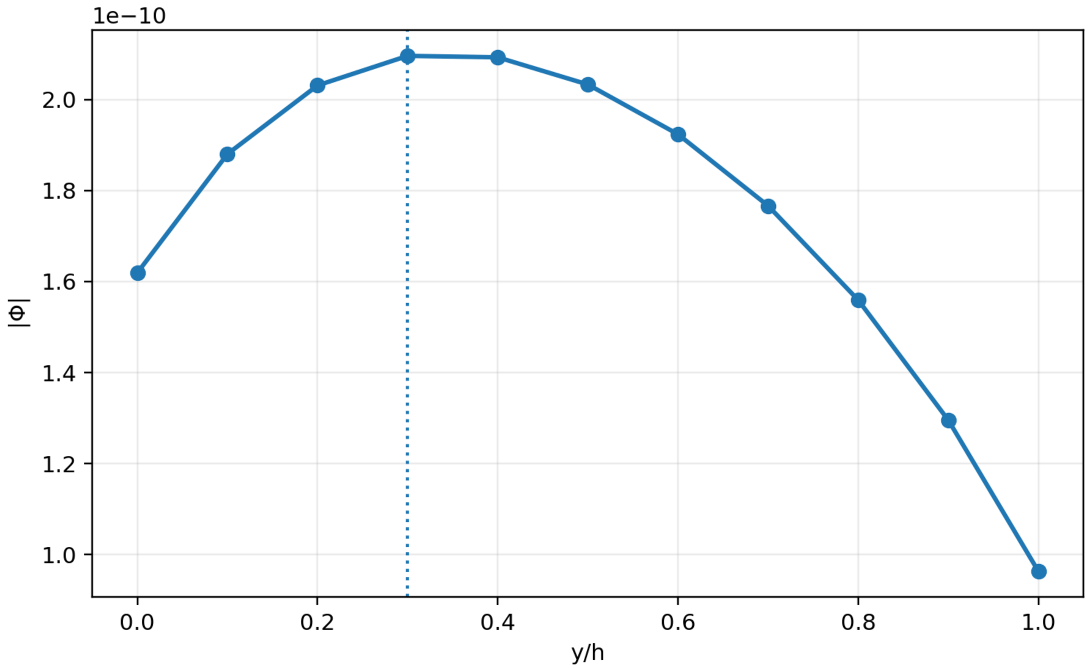

Figure 4. Microrotation amplitude through the layer; the maximum occurs near $y/h \approx 0.30$ for the reference case.

5.6 Couple-Stress Response

The couple-stress field is generated by gradients of microrotation and therefore represents a mechanical quantity that has no direct counterpart in classical elasticity. The corresponding couple-stress profile is shown in Figure 5.

For the present formulation, the couple-stress component associated with the microrotation gradient is

$$m_{yz} = \gamma\, \partial\Phi/\partial y$$

The numerical response demonstrates that couple stresses are controlled by the microrotational field and the intrinsic material parameters. They provide an additional mechanism for transmitting rotational interactions through the material.

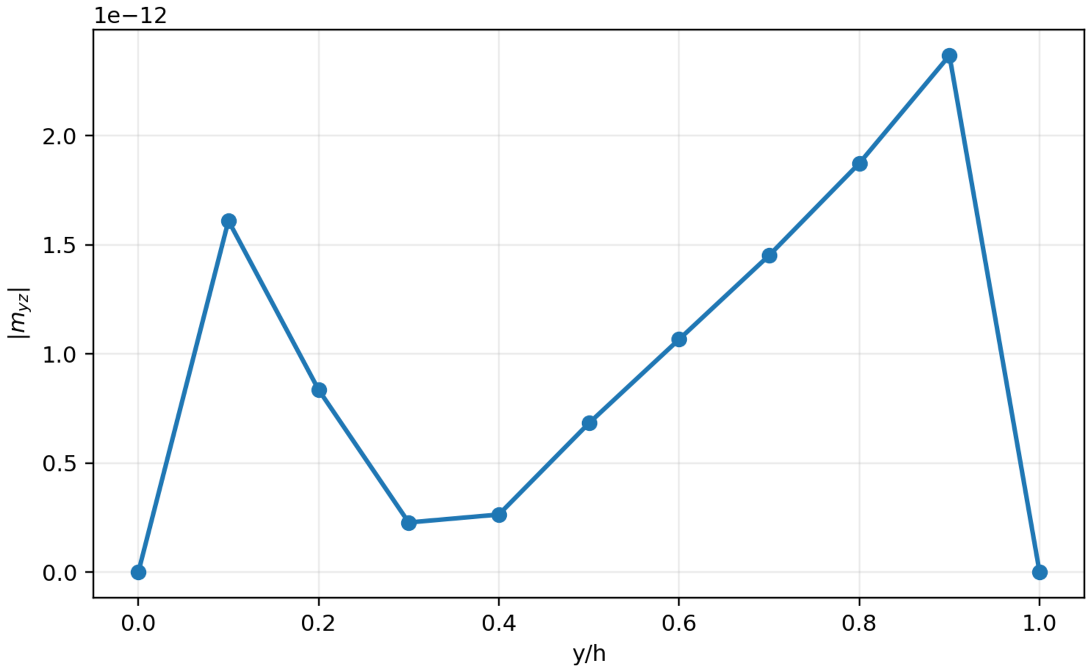

Figure 5. Couple-stress magnitude m_yz through the finite layer for the reference case.

5.7 Influence of the Micropolar Coupling Parameter

The coupling modulus controls the interaction between translational deformation and independent microrotation. Increasing this parameter is expected, within the governing micropolar formulation, to modify the coupled displacement and stress response.

For the present paper, this statement is retained as a qualitative interpretation of the model; no independent numerical sweep of the coupling modulus is used here to assign a quantitative trend.

5.8 Influence of Frequency

The excitation frequency enters the inertial terms of the stationary formulation and therefore affects both translational and rotational responses.

The present reference calculation demonstrates the response at the selected frequency, but no independent frequency sweep is used in this paper to establish a quantitative frequency trend.

Accordingly, statements concerning increased frequency sensitivity, modified attenuation, or the relative importance of additional rotational modes are treated as theoretical implications of the formulation rather than as independently verified numerical findings.

5.9 Influence of Characteristic Length

The characteristic length provides a measure of the scale associated with the micropolar rotational response.

Its role follows directly from the constitutive and characteristic relations of the formulation.

No independent characteristic-length sweep is included in the present numerical results; therefore, no quantitative trend with characteristic length is asserted here beyond its established theoretical role.

5.10 Classical Elasticity as a Limiting Case

An essential consistency test is obtained by suppressing the micropolar coupling and rotational effects. In the appropriate limiting formulation, the micropolar governing equations reduce to the corresponding classical elastic equations. This limiting relation provides a theoretical consistency check on the formulation and is consistent with the established classical elasticity and micropolar frameworks [1]–[6].

The present paper treats this limiting relation as a theoretical consistency condition; a separate numerical limiting-case calculation is not used as an independent quantitative result.

VI. Engineering Implications and Conclusions

6.1 Engineering Implications

The analytical and numerical results demonstrate that micropolar elasticity provides a more comprehensive description of microstructure-dependent mechanical behavior than classical elasticity because it incorporates independent microrotation and couple stresses.

The formulation is potentially relevant to micro- and nano-scale structures, layered composites, granular materials, cellular solids, acoustic metamaterials, MEMS/NEMS devices, vibration-isolation systems, and other materials in which rotational interactions and intrinsic length scales are mechanically important.

The developed analytical solution can also serve as a benchmark for validating numerical formulations, including finite-element and other computational approaches, because it provides a direct relation between material parameters, characteristic modes, boundary conditions, and measurable field quantities.

6.2 Conclusions

A unified analytical framework has been developed for stationary oscillation problems in isotropic micropolar elasticity using the Fourier integral transform. The formulation incorporates displacement, microrotation, force stresses, and couple stresses within a single mathematical framework.

The principal conclusions are:

1. The Fourier integral transform provides an effective means of reducing the coupled governing partial differential equations to a system of ordinary differential equations in the layer-normal coordinate.
2. The transformed problem can be represented by the characteristic matrix
   whose determinant produces a sixth-order characteristic equation and six characteristic roots.
3. The complete transformed solution is constructed from six characteristic modes and their associated modal vectors.
4. The finite-layer boundary-value problem is represented by an independent boundary matrix
   thereby avoiding ambiguity between the characteristic and boundary matrices.
5. The numerical reference case demonstrates substantial differences between micropolar and classical displacement responses.
6. The computed displacement profile in the finite layer is non-monotonic for the selected reference parameters and should not be interpreted as a simple monotonic attenuation law.
7. The micropolar formulation produces an independent microrotation field and corresponding couple stresses, which are absent from classical elasticity.
8. The coupling modulus, curvature-related parameters, characteristic length, and excitation frequency influence the translational and rotational responses in coupled but distinct ways.
9. The micropolar formulation recovers classical elasticity in the appropriate limiting case, providing an important consistency check.
10. The analytical formulation provides a useful benchmark for numerical simulations and for the analysis of engineering materials in which microstructural length scales and rotational interactions are significant.

6.3 Limitations and Future Work

The present formulation is restricted to homogeneous, isotropic, linear micropolar elasticity under small deformation and harmonic loading. The effects of material damping, thermal coupling, nonlinear constitutive behavior, and anisotropy are outside the present scope.

Future work may extend the formulation to multilayered and functionally graded micropolar media, thermo-micropolar and coupled-field problems, nonlinear material behavior, and experimental validation. Numerical implementations such as finite-element and boundary-element formulations can also be developed using the present analytical solution as a benchmark.

References

The reference list is retained from the working paper, with the established numbering:

[1] A. E. H. Love, *A Treatise on the Mathematical Theory of Elasticity*, 4th ed., Cambridge University Press, 1927.
[2] I. S. Sokolnikoff, *Mathematical Theory of Elasticity*, 2nd ed., McGraw-Hill, 1956.
[3] L. D. Landau and E. M. Lifshitz, *Theory of Elasticity*, 3rd ed., Butterworth-Heinemann, 1986.
[4] A. C. Eringen, "Linear Theory of Micropolar Elasticity," *Journal of Mathematics and Mechanics*, vol. 15, no. 6, pp. 909–923, 1966.
[5] A. C. Eringen, "Theory of Micropolar Elasticity," in *Fracture*, vol. II, H. Liebowitz, Ed. Academic Press, 1968, pp. 621–729.
[6] A. C. Eringen, *Microcontinuum Field Theories I: Foundations and Solids*. Springer, 1999.
[7] W. Nowacki, *Theory of Micropolar Elasticity*. Springer, 1975.
[8] I. N. Sneddon, *The Use of Integral Transforms*. McGraw-Hill, 1972.
[9] A. D. Polyanin and A. V. Manzhirov, *Handbook of Integral Equations*, 2nd ed. CRC Press, 2008.
[10] S. K. Tomar, "Wave Propagation in a Micropolar Elastic Plate with Voids," Journal of Vibration and Control, vol. 11, no. 6, pp. 849–863, 2005, doi: 10.1177/1077546305054788.
[11] A. C. Eringen, "Plane Waves in Nonlocal Micropolar Elasticity," International Journal of Engineering Science, vol. 22, nos. 8–10, pp. 1113–1121, 1984, doi: 10.1016/0020-7225(84)90112-5.

[12] B. Singh, "Wave Propagation in an Orthotropic Micropolar Elastic Solid," International Journal of Solids and Structures, vol. 44, nos. 11–12, pp. 3638–3645, 2007, doi: 10.1016/j.ijsolstr.2006.10.008.
[13] B. Singh and M. Goyal, "Wave Propagation in a Transversely Isotropic Microstretch Elastic Solid," *Mechanics of Advanced Materials and Modern Processes*, 2017.
[14] I.-D. Ghiba, G. Rizzi, A. Madeo, and P. Neff, "Cosserat Micropolar Elasticity: Classical Eringen vs. Dislocation Form," arXiv:2206.02473, 2022.
[15] N. M. Francis, R. A. Lebensohn, F. Pourahmadian, and R. Dingreville, "Micropolar Elastoplasticity Using a Fast Fourier Transform-Based Solver," International Journal for Numerical Methods in Engineering, vol. 126, no. 1, e7651, 2025, doi: 10.1002/nme.7651.
[16] M. Bhat and S. Manna, "Refining Boundary Value Problems in Non-local Micropolar Mechanics," 2024.